Journal of Machine Engineering, 2023, Vol. 23, No. 3, 5–25
ISSN 1895-7595 (Print) ISSN 2391-8071 (Online)

Received*: 23 June 2023* / Accepted: *24 July 2023* / Published online: *29 August 2023*

machine tools, precision, safety, sustainability

Eckart UHLMANN[1,2*]

RECENT ADVANCES IN PRECISION, SUSTAINABILITY AND SAFETY OF MACHINE TOOLS

Machine tools are the main driver of economic, environmental and social sustainability in industrial production. The ongoing shift from mass production to highly individualized, small batch manufacturing requires machine tools to be more flexible to changing needs while maintaining at least the same level of productivity. However, flexibility and productivity are at odds with the necessity for resource and energy efficiency. At the same time, more sophisticated workpiece specifications are pushing the boundaries regarding precision and dynamics of machine tools. In such a high-performance context, machine safety plays a major role and is becoming increasingly challenging due to higher kinetic energies of moving components. This paper examines recent advances in machine tool precision, sustainability, and safety. Six comprehensive case studies are provided to illustrate how these improvements contribute to an increased productivity. Hardware and software solutions for pose-controlled robotic manufacturing and thermoelectrically tempered high-performance spindles will be presented. Modular machine tool frames based on building blocks and an adaptive cooling system with thermoelectric generators for linear direct drives demonstrate their major impact on resource and energy efficiency. Machine safety is addressed through an analysis of potential hazards as well as improved protective measures. Model-based predictions precisely identify critical process parameters that lead to unbalance-induced failure of slim tool extensions, while on the protection side, new statistical models are applied to assess the protective performance of safeguards much more accurately. The cutting-edge technologies for machine tools presented in this paper will help manufacturers to cope with current and future challenges in industrial production.

1. INTRODUCTION

Productivity is fundamental to competitiveness and a key indicator of the success of any company. It can be defined as a measure of the efficiency of one or more factors of production in terms of the output-input ratio. In addition to the economic motivation, high productivity has become a necessity due to the ever-increasing world population and the need to make the most efficient use of available resources. The world's population has doubled in the last 50 years to over eight billion [1]. Over the same period, the proportion of people living in urban areas has increased from about 30% to over 50% and is still rising [2]. As a consequence, the limited space in urban areas goes hand in hand with a significant increase in the value

[1] Institute for Machine Tools and Factory Management IWF, TU Berlin, Germany
[2] Institute for Production Systems and Design Technology IPK, Fraunhofer, Germany
[*] E-mail: eckart.uhlmann@iwf.tu-berlin.de
https://doi.org/10.36897/jme/169941

of the "production area" as a resource. At the same time, the demand for products is growing, driven by the world's population and ongoing globalization. A recent example of rising product demand is the consumer electronics market. Annual smartphones sales, for example, have tripled in the last decade to nearly 1.4 billion units [3]. With about four billion smartphone users worldwide [4], the average life cycle of each device is less than three years. Short lifecycles are accompanied by the megatrend of individualization, which is reflected in consumer behavior and customer demand for personalized products. As a result, companies must be able to operate with high productivity in limited production areas with minimal use of resources, while responding flexibly to rapidly changing requirements.

Machine tools as the key component of industrial production play a crucial role in facing such demanding challenges. They must be more universally applicable or adaptable in order to save resources in terms of investment costs, material consumption and production space. In addition, the increasing demand for workpieces with multiple integrated functions is driving the need for high-precision machine tools to meet all tolerance classes of a part [5]. Based on this, the high precision of machine tools is directly linked to zero-defect manufacturing, which is essential for reducing the carbon footprint, saving resources and thus increasing productivity. Machine tool accuracy is determined by many factors, including the thermal behaviour and stiffness of machine tools [6–8]. This paper presents two novel approaches to high-precision manufacturing. The first is concerned with the thermal behaviour of machine tools, which is responsible for up to 75% of machining errors [6]. Uhlmann et al. [7] showed that a precise control of the machine tool temperature is required to produce high-precision parts with low variation. A thermoelectric temperature control system for motorized milling spindles that meets these requirements is presented. The presented system allows a significantly reduced warm-up time t_W, which leads to a major reduction of auxiliary process time in high-precision manufacturing and thus has a positive effect on productivity. The second approach deals with the application of industrial robots to manufacturing processes requiring high accuracy. Industrial robots will play a crucial role in the efficient manufacturing of individualized products [9]. However, the low precision resulting from the open kinematic chain still prevents their use for most manufacturing tasks. An approach based on artificial intelligence is presented, which captures the pose-dependent, nonlinear stiffness behaviour of industrial robots and, based on this, enables compensation of tool displacements during the process.

High-performance technologies that increase productivity in terms of higher output volumes are crucial to cope with rising product demands. At the same time, increased productivity goes hand in hand with the efficient use of resources, which is also a significant contribution to achieving the climate goals of the Paris Agreement [10]. For example, measures for more sustainable production include considering the energy consumption of the machine tool and reusing old machines with modular concepts [11]. Two novel approaches are proposed that address efficient material and energy use, respectively. Traditional cast or welded machine tool frames bind large amounts of material, making them inflexible and resource inefficient [12]. For an adaptive production environment, a modularized machine tool frame is presented that can be reconfigured on demand. At the same time, high productivity in terms of high-performance (HPC) and high-speed cutting (HSC) leads to significantly increased energy consumption and resulting heat losses [5]. In fact, the resulting

need for machine tool temperature control is the largest driver of energy consumption in machine tools [13]. To counteract this, an approach for an energy self-sufficient cooling system based on thermoelectric generators (TEG) for linear direct drives (LDD) in HPC and HSC machine tools is presented.

High feed rates v_f and rotational speeds n in highly productive HPC and HSC machining operations also require significantly increased safety precautions along the entire cause-effect chain due to the stored kinetic energy. Experimental investigations of machine safety are increasingly extended by the development of numerical and statistical models. This paper presents a model-based identification of the elevated risk potential associated with the use of slim tool extensions (STE) using finite element (FE) simulations. Furthermore, novel statistical models to accurately assess the protective performance of safeguards are discussed.

In conclusion, the machine tools of the future will be highly productive, have increased precision for the manufacture of function-integrated parts, be sustainable in terms of resource and energy efficiency, and meet strict safety requirements. In 2015, the United Nations adopted the 2030 Agenda, which includes 17 Sustainable Development Goals (SDG). The 17 SDGs include, in particular, ending poverty and hunger, protecting human rights, building global partnerships, increasing prosperity for all, as well as addressing inequality and climate change [14]. In all disciplines, the impact on specific SDGs should be used as the key criterion for evaluating research and developments results. The cutting-edge technologies presented in this paper address a productivity increase in the sense of precision, sustainability and safety, which take a positive influence on the SDGs “decent work and economic growth” (SDG 8), “industry innovation and infrastructure” (SDG 9), “responsible consumption and production” (SDG 12) as well as “climate action” (SDG 13).

The remainder of the paper is divided into four chapters. Chapter 2 presents recent research advances in precision through thermoelectrically tempered motorized milling spindles and high-precision robot manufacturing. Chapter 3 is dedicated to sustainability in production. Modularization of machine tool frames with building blocks and energy self-sufficient cooling systems are discussed as two major contributions to energy and resource savings. Chapter 4 focuses on machine safety in terms of slim tool extensions and safeguards. A conclusion is given in Chapter 5.

2. PRECISION OF MACHINE TOOLS

2.1. THERMOELECTRICALLY TEMPERED MOTORIZED MILLING SPINDLE

Applications in optics, metrology, automotive, and information and communications technology require machined components with submicron shape and position tolerances [7]. Manufacturing high-precision components in large quantities is challenging and requires a sufficient productivity. During machining, thermally induced shifts Δl_{th} of the positional correlation between tool and workpiece have a significant influence on the machining accuracy of machine tools [6]. This is due to electrical and mechanical power losses ΔP_J, which induce significant heat flow rates $\dot{Q}_{ind}$ in machine tool components [6]. The drives and

bearings of motorized milling spindles are one such significant heat source. Due to their proximity to the tool center point (TCP), motorized spindles have a considerable influence on the achievable machining accuracy of machine tools. To minimize the negative impact on the achievable machining accuracy, the thermal losses must be dissipated by effective cooling systems. Denkena et al. [15] present a comprehensive overview of various relevant cooling systems for motorized spindles. Most approaches, especially commercially available fluid cooling systems, provide effective heat dissipation but do not respond to changes in the induced heat flow rates $\dot{Q}_{ind}$. These changes are, however, unavoidable and are caused, for example, by changes in rotational speed n, load torque M_l or machine downtime t_0 as a result of tool or workpiece changes [13]. Consequently, any change in the induced heat flow rates $\dot{Q}_{ind}$ leads to a change in the steady state temperature ϑ_s. The warm-up time t_w required to reach this thermal steady state is time-consuming and has a negative impact on productivity.

One possibility to control the heat dissipation of the cooling system and thereby the spindle temperature ϑ_{sp} is to control the temperature ϑ_f or the volumetric flow rate $\dot{V}_f$ of the cooling fluid [16]. Another approach is to use thermoelectric-based cooling systems [15, 16]. Furthermore, Jonath et al. [16] present a heat pipe based tempering system to control the spindle temperature ϑ_{sp}.

In order to improve the thermoelastic behaviour of machine tools, and in particular to reduce the warm-up time t_w after machine downtime t_0, a prototype of a thermoelectrically tempered motorized spindle has been developed and manufactured by the Institute for Machine Tools and Factory Management IWF and the Alfred Jäger GmbH [17]. Fig. 1 shows a model of the prototype spindle with six Peltier modules arranged around the front and rear bearings, respectively, as well as twelve Peltier modules arranged around the stator of the motor.

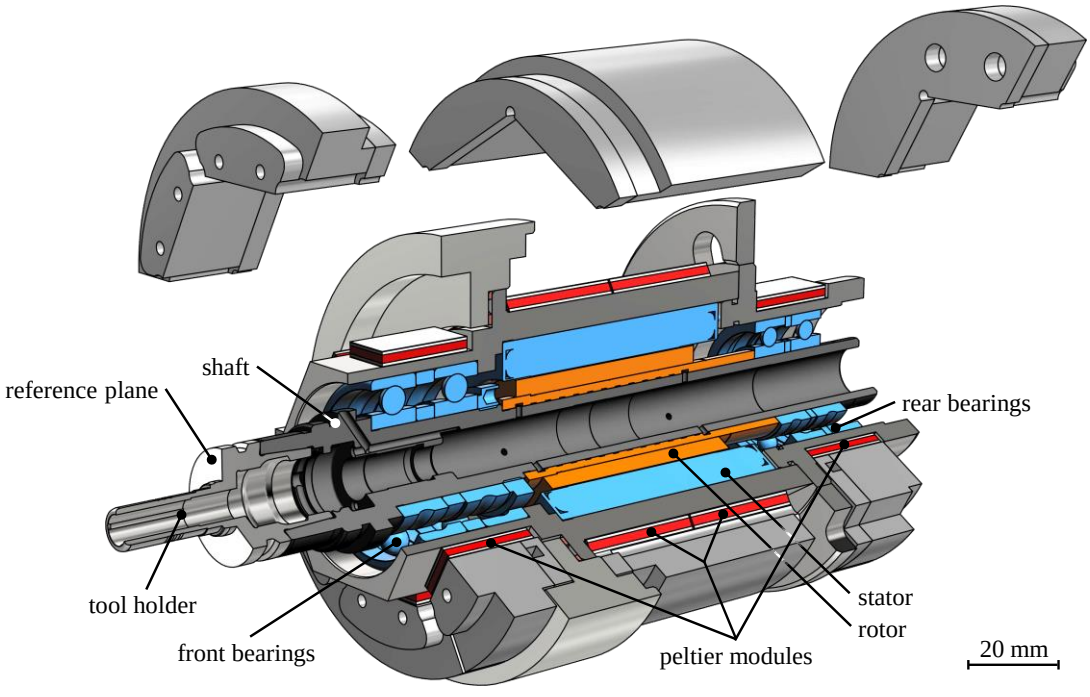

Fig. 1. Model of a thermoelectrically tempered motorized milling spindle

The Peltier modules are able to pump heat depending on the electrical Peltier current I_{Pel}. A closed control loop makes it possible to control the bearing temperatures ϑ_b on the outer rings and the stator temperature ϑ_{st} on the outer stator surface. An external capacitive displacement sensor allows the measurement of the axial shaft elongation Δl_s at a reference plane on the tool holder.

To show the potential of the thermoelectric temperature control system the spindle prototype was compared with a commercial reference spindle of type Z62-H360.02 made by Alfred Jäger GmbH, Ober-Mörlen, Germany. Both spindles were run on a test bench with measurement of the axial shaft elongation Δl_s. In the test procedure, both spindles were driven at a rotational speed n = 55,000 1/min and stopped for a downtime $t_0 \approx 300$ s to simulate a tool or workpiece change.

Figure 2a shows the axial shaft elongation Δl_s of the reference spindle. The reference spindle shows an average axial shaft elongation $\overline{\Delta l_s}$ = 20.7 µm at a rotational speed n = 55,000 1/min. With the spindle at standstill, the axial shaft elongation Δl_s decreases immediately and over the entire downtime t_0, the axial shaft elongation Δl_s decreases continuously. After setting the rotational speed back to n = 55,000 1/min, the axial shaft elongation Δl_s reaches a steady state after a warm-up time t_W = 343 s.

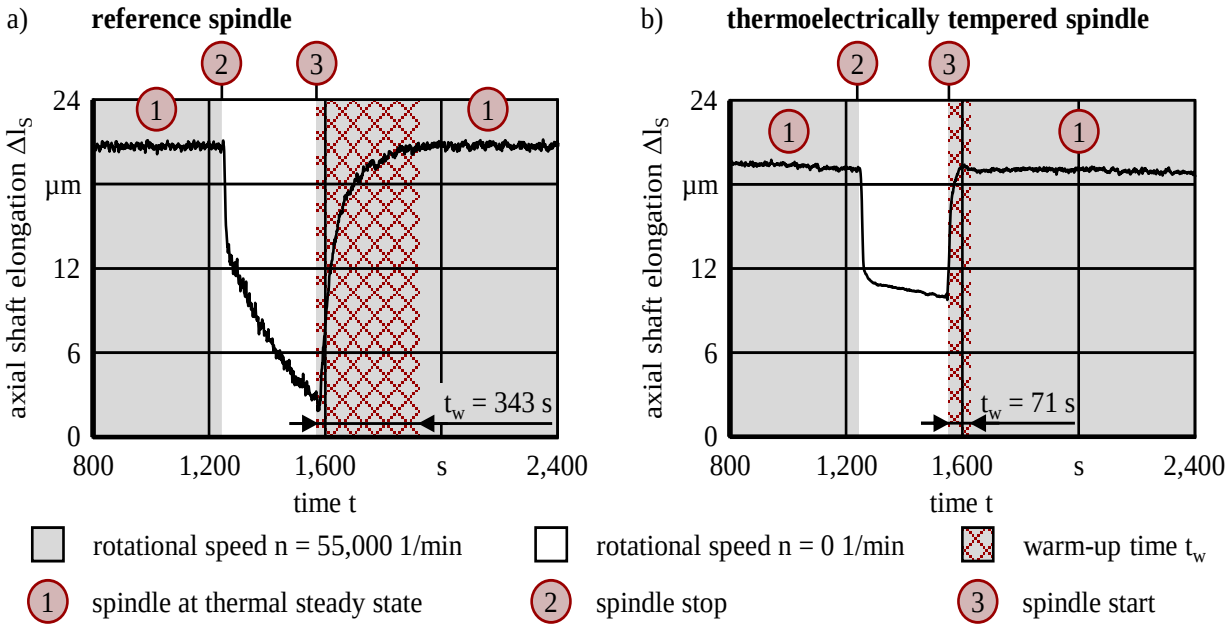

Fig. 2. Measurement of axial shaft elongation Δl_s; a) reference spindle of type Z62-H360.02; b) prototype of a thermoelectrically tempered spindle

In the prototype spindle the thermoelectric tempering system allows to control the front bearing temperature $\vartheta_{b.f}$, the rear bearing temperature $\vartheta_{b.r}$ and the stator temperature ϑ_{st}. All temperatures are set to $\vartheta_{b,f} = \vartheta_{b,r} = \vartheta_{st} = 25°C$ while the spindle is operating. During the downtime t_0 the temperature of the front bearing is set to $\vartheta_{b,f} = 37°C$. Figure 2b shows the axial shaft elongation Δl_s of the thermoelectrically tempered spindle. The average axial shaft elongation is $\overline{\Delta l_s}$ = 19.0 µm at a rotational speed n = 55,000 1/min. When stopped, the axial

shaft elongation Δl_s also decreases immediately. As a result of the controlled heating, the continuous reduction of the axial shaft elongation Δl_s is much lower than that of the reference spindle. Setting the rotational speed back to n = 55,000 1/min, the axial shaft elongation Δl_s reaches a steady state after a warm-up time t_w = 71 s.

The results presented in Fig. 2 show that the thermoelectric tempering system can affect the axial shaft elongation Δl_s of the spindle. It is shown that the warm-up time t_w to reach a thermal steady state of the axial shaft elongation Δl_s after a machine downtime t_0 can be significantly reduced. In this particular case, a 79% reduction in the warm-up time t_w is achieved. This reduced warm-up time t_w leads to a major reduction in auxiliary process time in the field of high-precision manufacturing and thus has a positive effect on productivity.

2.2. HIGH-PRECISION ROBOT MANUFACTURING

The accumulation of uncertainties along the serial kinematic chain of industrial robots results in low absolute positional accuracies AP of the TCP, which still prevents robot manufacturing in case of e. g. robot machining or robot forming on an industrial scale. However, substituting conventional machine tools by industrial robots constitutes a significant step towards high productivity in an adaptable production, especially due to their large available workspace, six or more degrees of freedom, and a generalized end-effector control. Therefore, increasing the absolute positional accuracy AP of industrial robots has been an open field of research for many years. The approaches are mainly based on:

- robot design, e. g. with novel hybrid serial-parallel kinematic chains [18] and direct or hybrid drives [19];
- robot control, e. g. double encoders [20], visual servoing [21], and force control [22];
- robot calibration, e. g. by improving the modelling, parameter identification and compensation methods [23, 24], and
- artificial intelligence (AI), e. g. data-driven modelling and compensation [25, 26].

The latter in particular is gaining increasing attention due to the digitization of industry and the resulting connectivity of machines with large data streams. Uhlmann et al. [25] presented a framework to obtain optimal Artificial Neural Networks (ANN) to increase the absolute positional accuracy AP of industrial robots using hyperparameter optimization. The ANN model maps the six joint angles $\boldsymbol{\theta}$ at the input to the six-dimensional absolute or relative pose vector $\boldsymbol{p}$ at the output. Various aspects such as learning and extrapolation capabilities were examined. Blumberg et al. [26] continued the work and added the external force $\boldsymbol{F}$ as an input parameter to the model. Based on tis, the stiffness behaviour of industrial robots is captured in terms of the six-dimensional tool deflection $\boldsymbol{u}$. Besides ANN, Gaussian Process Regression (GPR) is investigated as an alternative modelling approach, which proves to be superior with respect to generalization with small data sets.

To train such an AI model in a supervised learning context, the input-output relationships must be determined experimentally. The measured outputs – so-called labels – are compared to the model predictions, with the difference being fed back as an error function to optimize the model parameters. The trained AI model can be used to predict tool

deflections $\boldsymbol{u}$ of an industrial robot along a toolpath for an arbitrary task. A compensated toolpath is obtained by iteratively adjusting the joint angles $\boldsymbol{\theta}$ based on the predicted tool deflections $\boldsymbol{u}$ and a kinematics model of the industrial robot. The iteration stops when the path deviation is below a threshold. The model training and model-based compensation strategies are summarized in Fig. 3.

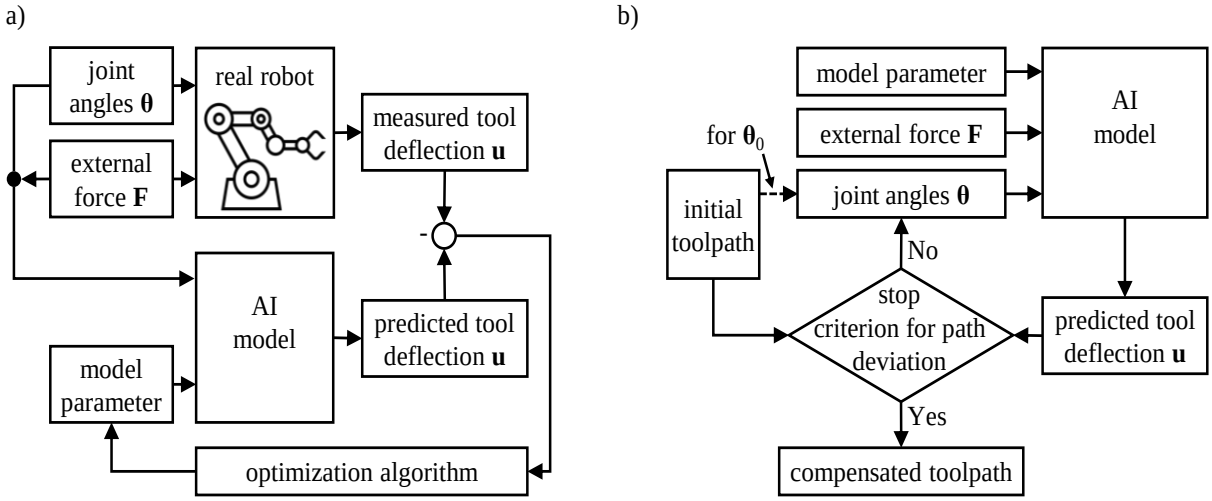

Fig. 3. Data-driven model to increase the absolute positional accuracy AP of industrial robots; a) model training; b) model-based compensation

Robot-based hole flanging by single point incremental forming (SPIF) with the industrial robot M-900iB/700 by the company Fanuc K.K., Oshino, Japan, is used to validate the effectiveness of the proposed training and compensation strategies. Hole flanging is the process of expanding pre-cut holes in blanks to form flanges and is part of the process chain in the manufacture of many sheet metal parts. SPIF's addition of hole flanging makes the process more flexible and reduces costs by eliminating the need for dedicated forming equipment. [27]. Using industrial robots as manipulators further increases flexibility and provides opportunities to form flanges in hard-to-reach areas with novel process strategies such as overbending as well as inclined or undercutted flanges [28, 29]. However, due to the low stiffness of industrial robots, the process force $\boldsymbol{F}_p$ causes unwanted tool deflections $\boldsymbol{u}$ and results in low machining accuracies. To model the tool deflection $\boldsymbol{u}$ in terms of an AI model, the industrial robot is moved on different loaded and unloaded circular tool paths, for which the joint angles $\boldsymbol{\theta}$ and the external force $\boldsymbol{F}$ are recorded at discrete points. The tool deflection $\boldsymbol{u}$ follows as the difference between the absolute pose $\mathbf{p}$ with and without the applied external force $\boldsymbol{F}$, which is measured by the lasertracker AT960 in combination with a T-MAC sensor from Hexagon AB, Stockholm, Sweden. A total of $N = 352$ data points are obtained experimentally.

The trained AI model is used to calculate compensated tool paths based on the initial tool path and the known – measured or simulated – process force $\boldsymbol{F}_\mathrm{p}$ in hole flanging by SPIF, see Fig. 4. The compensated toolpaths are experimentally validated with sheet blanks made of Aluminum EN AW-6181-T1 with a sheet thickness of $s = 0.8$ mm. Holes with a pre-cut diameter of $D_0 = 25$ mm were milled in the centre of the blanks before the forming operation. The target diameter of the flange is $D = 40$ mm. The validation experiments are performed

for two different positions in the workspace of the industrial robot to account for the pose dependency of the robot stiffness. The flange diameter is measured posterior with a 3D measurement gauge. Figure 4 gives an overview of the experimental validations and results. The machining accuracy of the flanges is improved by 75% from a maximum deviation from the target diameter D of δ_{unc} = 2.4 mm without compensation to δ_{com} = 0.6 mm with compensation. At the same time the differences between the minimum and maximum measured flange diameters, D_{min} and D_{max}, are reduced with the compensation strategy, resulting in more circular flanges.

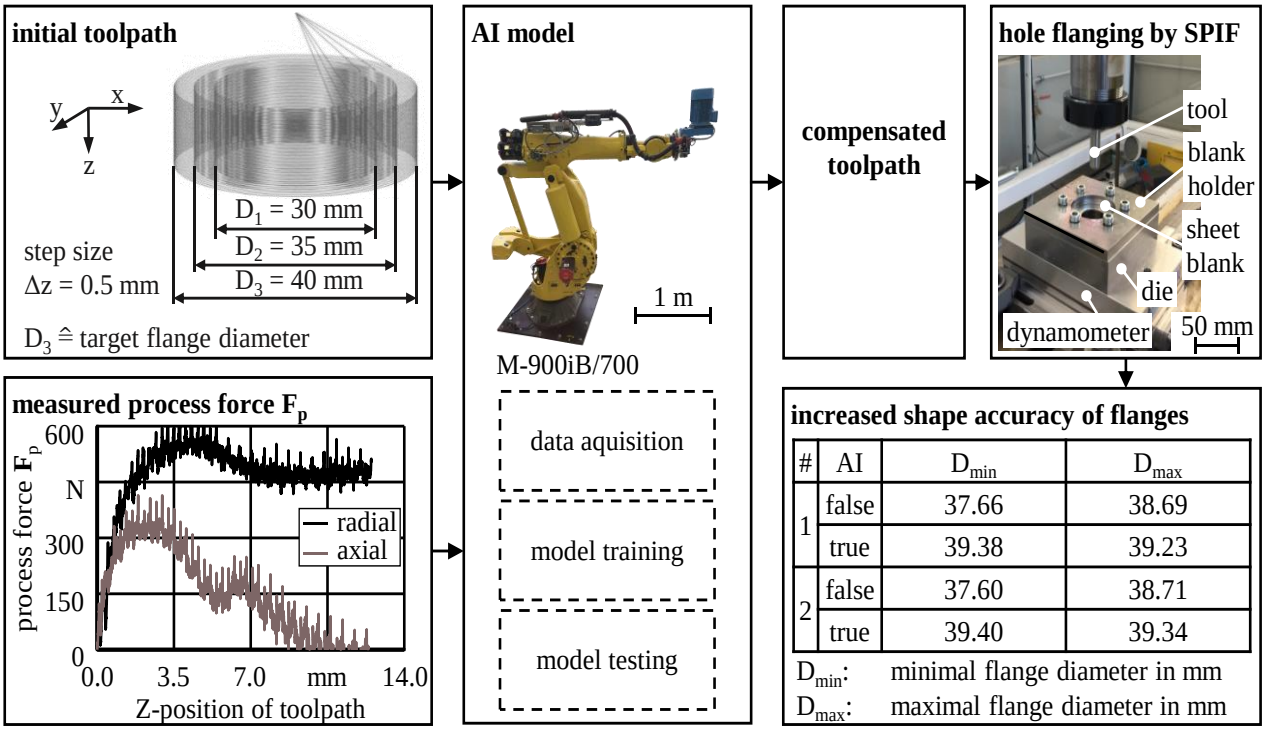

Fig. 4. Experimental validation of the data-driven compensation based on hole flanging by SPIF

In summary, the partial substitution of machine tools by industrial robots will play a substantial role in meeting individualized product requirements at high absolute volumes. In this context, industrial robots will have to satisfy a higher level of precision. Conventional methods based on robot calibration are not able to meet such accuracy requirements due to nonlinearities in the system behaviour, backlash and friction in the joints, as well as wear. Increasing digitization and connectivity in manufacturing supports the availability of large data streams. AI-based regression models have the potential to detect physical patterns in large data streams and thus contribute significantly to improving the accuracy of industrial robots. In this paper, it has been shown that for an application in robot-based hole flanging by SPIF the machining accuracy of formed flanges can be increased by up to 75% by means of an AI-based compensation of tool deflections $\boldsymbol{u}$. The approach is by no means limited to SPIF hole flanging, but can be applied to any robotic application where high precision is important.

3. SUSTAINABILITY OF MACHINE TOOLS

3.1. MODULARIZED MACHINE TOOL FRAME BASED ON BUILDING BLOCKS

Manufacturing companies are facing significant challenges due to increasing customer demands for product variants with small lot sizes and short time-to-market. Realizing resource-efficient machine tools with long lifecycles requires therefore high flexibility and adaptability with respect to changing requirements. One promising approach relies on so-called reconfigurable manufacturing systems (RMS), which Koren [30] defines as systems for fast adaptation of the production capacity and functionality by changing the structure as well as the hardware and software. Feng and Huang [11] discussed the sustainability benefits due to machine tool modularity over the entire product lifecycle. The sustainability gain is mainly due to the low variety, complexity and reuse of parts as well as the flexibility in the applications. The modularization required for RMS has already been advanced in many areas of machine tools, such as drives, tools, toolholders, and clamping systems [31]. However, machine tool frames, which provide the basic structural support for any machine tool, are still cast or welded structures that cannot be reconfigured. As a result, the overall adaptability of machine tools in terms of working area, spindle orientation, and manufacturing process remains limited. Brankamp and Herrmann [32] introduced the idea of Building Block Systems (BBS), which was intensively studied by Ito [33] with respect to modularized machine tools. Wulfsberg et al. [34] summarize different concepts of machine tool modularity in micro-production and present solutions for the scalability of the working area. Mori and Fujishima [31] designed a reconfigurable machine tool with axis modules that allow the spindle configuration to be changed between horizontal and vertical. Abele and Wörn [35] introduced the concept of reconfigurable multi-technology machine tools (RMM) to enable the integration of different manufacturing processes in a single workspace. However, in all approaches the modularization is done on a large scale, i. e. the resulting reconfiguration capabilities are limited to a few a priori built-in configurations making them inflexible to unknown changes in requirements. Uhlmann and Peukert [36, 37] introduced the concept of fine-scale building blocks for machine tool frames under the name of LEG²O. The hexagonal building blocks are topologically optimized to minimize mass and maximize stiffness, allowing a wide range of different configurations, see Fig. 5.

The exemplary gantry milling machine tool is realized as a prototype made of $z_f = 37$ full and $z_h = 10$ half hexagonal building blocks. In addition to the basic machine tool frame, the building blocks are used to build the crossbeam and to stiffen the z-axis. All axes are driven by synchronous motors with frequency converters and planetary gearboxes. The linear motions are realized by racks and linear guides. Both can be segmented and stacked together in order to scale the working area. The spindle HFP-D-10525-09 of Mechatron GmbH, Darmstadt, Germany, with a nominal power of $P = 2.5$ kW and a maximum rotation speed of $n = 9{,}000$ 1/min is installed. The dynamic behaviour of the prototype has been investigated by a modal and operating deflection shape (OPS) analysis, see Fig. 6.

The modal analysis is performed at the TCP by exciting a dummy tool with an electro-dynamic shaker. The response is measured with an accelerometer. Eigenfrequencies f_R and

damping D are identified from the frequency response function as shown in Fig. 6b for the first eight eigenmodes. The low eigenfrequencies f_R are a result of the reduced machine tool stiffness due to the numerous interfaces of connected building blocks. At the same time, the relative motions between surfaces in the contact area are the reason for large damping D. An OPS analysis further proves the potential of modularized machine tool frames as is shown in the stability lobe diagram in Fig. 6c. The analysis is performed with a stepped workpiece made of EN AW 7075 aluminum and a two-flute cemented carbide milling tool with a diameter of $d = 8$ mm. Process stability is assessed based on accelerations measured at the spindle in the frequency domain and the resulting surface roughness. Below an axial depth of cut of $a_p \leq 1.4$ mm the process remains stable regardless of the rotational speed n. In addition, there is a stable region within the examined limits above rotational speeds of $n \geq 6{,}125$ 1/min.

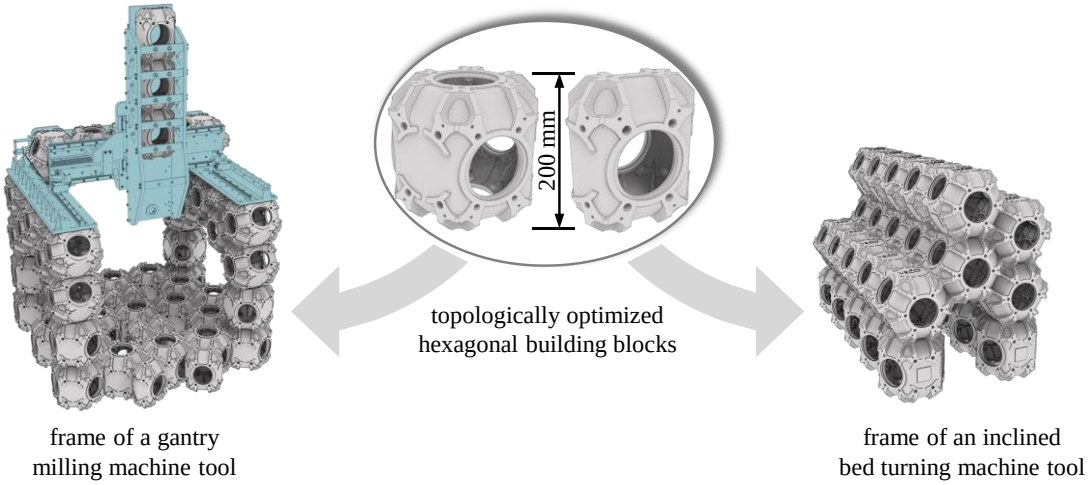

Fig. 5. Building blocks LEG²O with two exemplary machine tool frames

a)

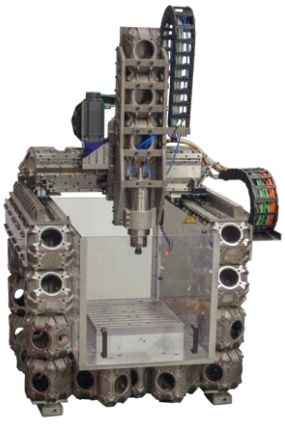

b)

i	1	2	3	4	5	6	7	8
eigenfrequency f_{Ri} in Hz	45	106	169	302	715	924	1,505	1,422
damping D_i in %	7.8	8.0	13.8	1.9	7.9	3.1	3.1	4.9

c)

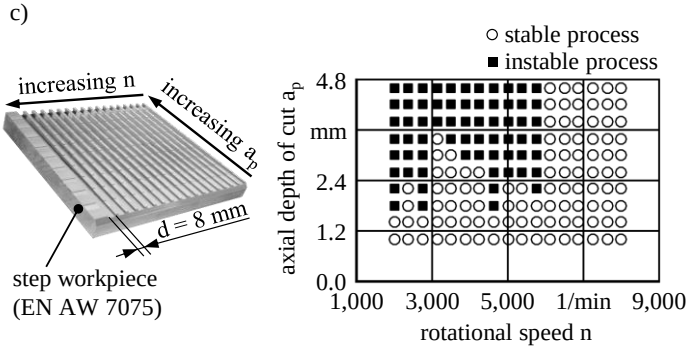

Fig. 6. Dynamic behaviour; a) prototype of the gantry milling machine tool based on the building blocks LEG²O; b) results of modal analysis; c) results of OPS analysis in terms of stability lobes

In conclusion, highly modularized on demand and can therefore be used to increase productivity in an adaptive manufacturing with continuously changing requirements. The demonstrator of a gantry milling machine tool based on LEG²O building blocks has shown that even a fine-scaled modularized machine tool frame can achieve industry-relevant stiffness behaviour and process characteristics. In future research actuated building blocks will be integrated into the structure to allow static, thermal and dynamic compensation of modularization deficits.

3.2. ENERGY SELF-SUFFICIENT COOLING SYSTEM FOR LINEAR DIRECT DRIVES

HPC and HSC are technologies used to realize higher output volumes and thus increase productivity. To realize the required feed rates v_f, linear direct drives (LDD) are commonly used in such machine tools. Due to the electrical power losses ΔP_J of the LDD, a significant heat flow rate $\dot{Q}_{ind}$ is induced in the adjacent components of the machine tool. Maintaining the required machining accuracy of machine tools, and thus reducing thermally induced displacements δ_{th} requires the installation of energy-intensive cooling systems, which account for a significant portion of the total energy consumption of machine tools [13]. With the intention to achieve a demand-oriented cooling, an *Adaptive Cooling (AC) system* with TEG was developed at IWF [38–42]. With the ability to convert a portion of the induced heat flow rate $\dot{Q}_{ind}$ into electrical energy E to supply electrical loads, a thermoelectrically driven cooling system has the potential to be energy self-sufficient.

Figure 7 shows the *AC system*, consisting of TEG integrated in the heat flow rate $\dot{Q}_{ind}$ between the primary part of the LDD and the water-cooled cold plate. The recuperated electrical power P_{el} corresponds to the difference between the absorbed heat flow rate $\dot{Q}_{abs,h}$ and the generated heat flow rate $\dot{Q}_{gen,c}$ at the hot and cold sides of the TEG, respectively, and is used to supply a water pump and a fan. Due to its direct connection to the machine slide, whose thermally induced deformations Δl_{th} can negatively affect the machining accuracy of machine tools, the connection plate is defined as the precision-related component of the assembly.

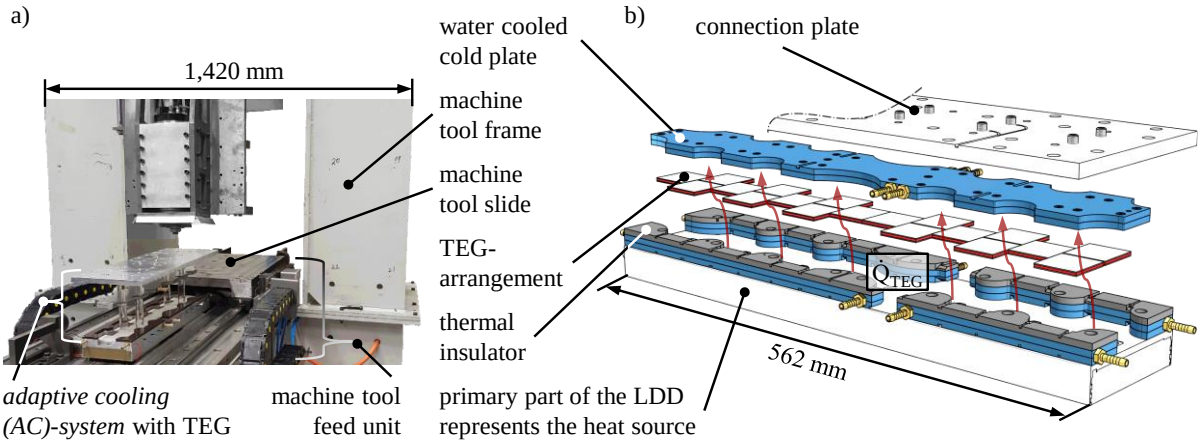

Fig. 7. *AC-system* with TEG; a) prototypical integration in a machine tool demonstrator with LDD; b) exploded view of the design

In order to conduct a significant portion of the heat flow rate $\dot{Q}_{ind}$ through the TEG into the water cooler and thus minimize the temperature rise of the connection plate, thermal insulators are inserted at the sides, Fig. 7b. The prototype *AC system* was integrated into the feed axis of a machine tool with LDA, Fig. 7a, and equipped with type K thermocouples made by Therma Thermofühler GmbH, Lindlar, Germany, for the acquisition of experimental data.

During the experimental studies, the following three modes of operation of the *AC system* are investigated:

1. a reference operating mode without active cooling, in which the *AC system* was turned off, Fig. 8,
2. a non-energy self-sufficient operating mode in which a compressor cooling unit, Typ Chilly-15 S, from Hyfra GmbH, Krunkel, Germany, was additionally used and powered with an externally supplied energy E_{ext}, Fig. 8, and
3. an energy self-sufficient operating mode, in which the cooling capacity P_C was completely generated by recuperated electrical power P_{el} from TEG, Fig. 8.

In the second and third operating mode, the recuperated electrical power P_{el} is fed directly into a parallel electrical circuit, consisting of a Typ P123001 gear pump distributed by Thermalforce GmbH, Berlin, Germany, within a water cooling circuit and a Typ 4412 fan made by Ebm–Past Mulfingen GmbH, Mulfingen, Germany, as part of a self-designed adiabatic air cooling unit, Fig. 8. With this configuration, the two electrical loads on the *AC system* are self-powered by TEG. In the third operating mode, the coolant inlet temperature ϑ_{in} is completely determined by the adiabatic air cooling unit. Due to the limited amount of recuperated electrical power P_{el}, the adiabatic air cooling unit with a fan is not able to provide coolant with a constant inlet temperature ϑ_{in}. In order to meet this requirement for the performance analysis of the *AC system*, the compressor cooling unit with a two-point controller is additionally used in the second operating mode, Fig. 8. This allows a closed-loop control of the coolant inlet temperature ϑ_{in} to a defined setpoint of $\vartheta_{\text{in}} = 22°\text{C}$ with a hysteresis $H = 1.4$ K, Fig. 8a. While using the compressor cooling unit, the fan of the adiabatic air cooling unit was rotating without cooling function.

The experimental results show that using the *AC system* with TEG in the second and third operating mode ensures a motor core temperature $\vartheta_M < 100°\text{C}$, thus allowing unrestricted usability of the LDA, Fig. 8a. Compared to the reference mode, the energy self-sufficient operation shows a significant reduction in temperature on top of the primary part ϑ_{pp} at the time $t = 1{,}350$ s, as well as a significantly reduced temperature rise $\Delta\vartheta_{pp}(t)$ in any time interval Δt, Fig. 8a. Furthermore, the temperature rise in the precision-related connection plate $\Delta\vartheta_{cp}(t)$ was significantly decreased compared to the reference operating mode, Fig. 8b. This improved thermal behaviour is due to the integrated TEG of the *AC system*, which recuperate enough electrical power P_{el} at the time $t \geq 200$ s to drive the water pump, as well as the parallel-connected fan of the adiabatic air cooling unit, Fig. 8c.

Compared to a conventional cooling system for LDD, the *AC system* has an increased global thermal resistance R_{gl}. This is because a significant portion of the induced heat flow rate $\dot{Q}_{ind}$ is forced through the additional thermal resistance R_{TEG} of the TEG arrangement. This results in a high temperature on top of the primary part ϑ_{pp} and thus a negative influence on the operability as well as the thermal stability. Further investigations showed, that implementing a primary and secondary heat path has the potential to reduce the global thermal

resistance R_{gl} and thereby to increase the performance of the *AC system* [43]. It has been shown that a 24.6% reduction in the temperature at the top of the primary part ϑ_{pp} and a 15.2% reduction in the temperature on the upper surface of the precision-related connection plate ϑ_{cp} can be achieved with this approach.

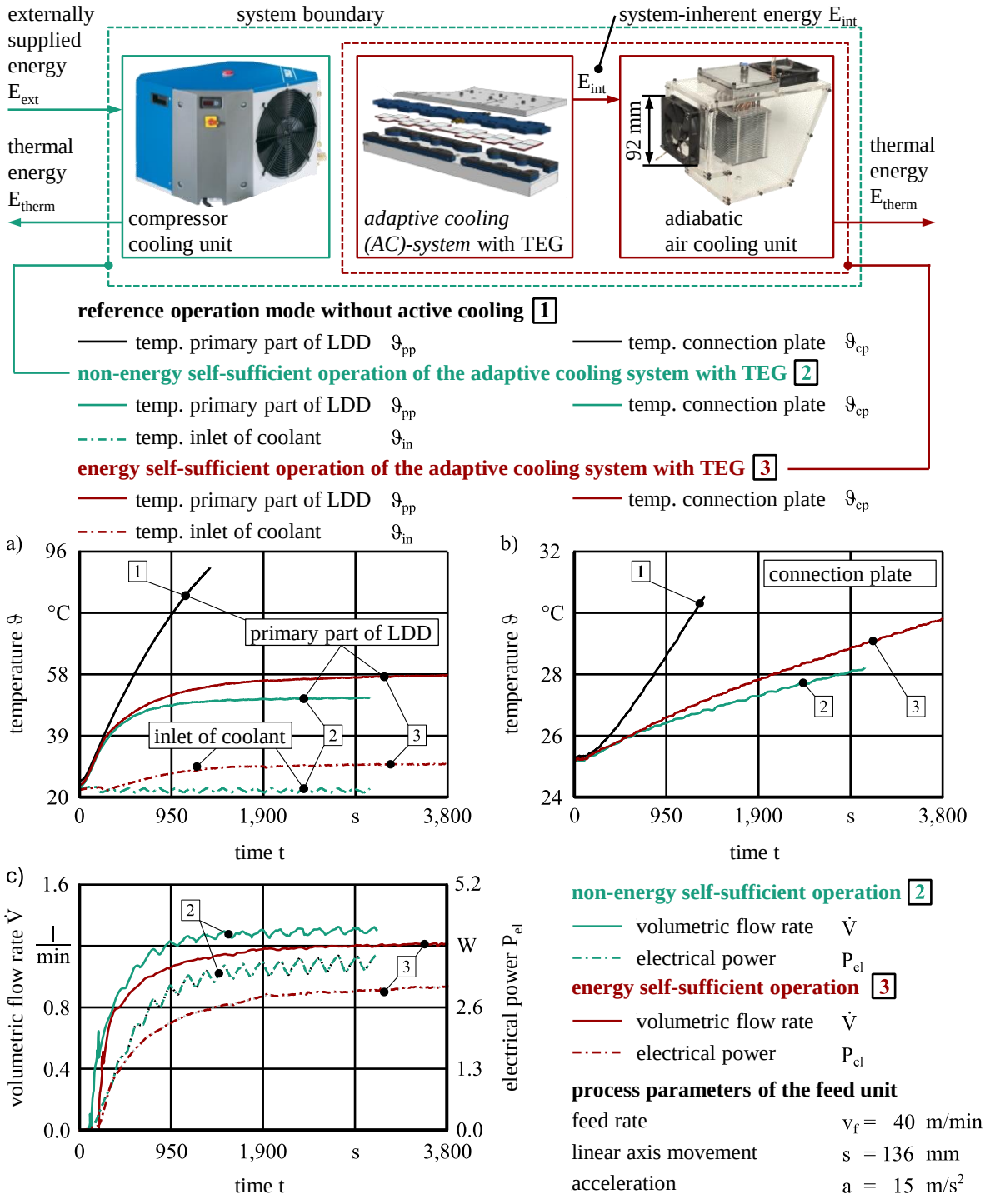

Fig. 8. AC system in three operating modes with an induced heat flow rate $\dot{Q}_{ind} \approx 700$ W; a) temperatures on top of the primary part ϑ_{pp} and inlet temperatures of the coolant ϑ_{in}; b) temperatures inside the precision-related connection plate ϑ_{cp}; c) volumetric flow rate $\dot{V}$ of coolant and recuperated electrical power P_{el} [40]

In the energy self-sufficient mode of operation, the *AC system* allows the unrestricted use of the LDD without the external electrical power P_{el} for cooling. In the case presented, this results in a saving of electrical power P_{el} = 800 W and an increase in productivity in terms of efficient energy use.

4. SAFETY OF MACHINE TOOLS

4.1. RISK ASSESSMENT OF SLIM TOOL EXTENSIONS FOR MILLING OPERATIONS

The demands on machine tool safety are constantly increasing as a result of productivity enhancements such as an increased feed rate v_f and rotational speed n in HPC and HSC machining. This trend is further accelerated by the need to reduce component weight. To address these challenges, the complete machining of components is becoming increasingly attractive [44]. As a result, 90% of aerospace parts are fully machined machined [45]. Under such conditions, the accessibility of the workpiece becomes more and more demanding. Slim tool extension (STE) solve the problem of a limited accessibility and allow complete machining of integral parts. Figure 9 shows a schematic design of a STE.

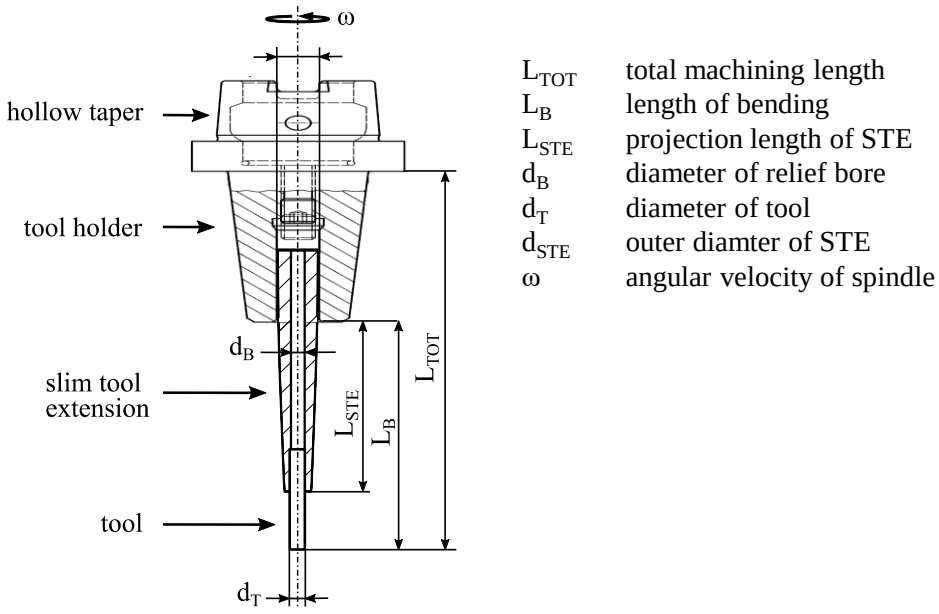

Fig. 9. Schematic of a STE clamped into a tool holder with tool attached [46]

From a safety perspective, however, STE are associated with an increased hazard potential. The elevated deflection $w(x)$ of long cantilevered STE due to plastic deformation leads to an increase in the eccentric mass of STE m_{STE}. Since machine tool spindles are generally speed-controlled, the effect described above results in increased kinetic energy E_{kin} of STE. However, a reassessment of the hazard potential and the derived safety measures to use STE in machine tools has not been performed due to the lack of adequate models for the

quantitative determination of such hazard potentials [47]. An elementary requirement for the design of safeguards is defined in ISO 14120 [48] and consists of the retention of ejected workpiece or tool fragments.

The maximum kinetic energy $E_{\mathrm{kin,max}}$ of such fragments is calculated according to Eq. (1), assuming a standard mass of m = 0.1 kg, where B is the maximum tool diameter and $n_{S,max}$ is the maximum spindle speed.

$$E_{\mathrm{kin,max}} = 1/2 \cdot m \cdot \left(B \cdot \pi \cdot n_{\mathrm{S,max}}\right)^2 \tag{1}$$

However, the assumptions of ISO 14120 [48] do not consider a possible higher kinetic energy E_{kin} due to an increased eccentric mass m_{STE} of the STE. Thom and Uhlmann [47] were the first to use FE simulations to investigate potential failure conditions and the associated increase in kinetic energy E_{kin} upon failure of the STE. The STE and attached tool were modelled as a cantilever Timoshenko beam with constant outer diameter d_{STE} and constant diameter of the relief hole d_B, using a bilinear kinematic hardening material model of the ductile metal X38CrMoV5-152^{+2} HRC.

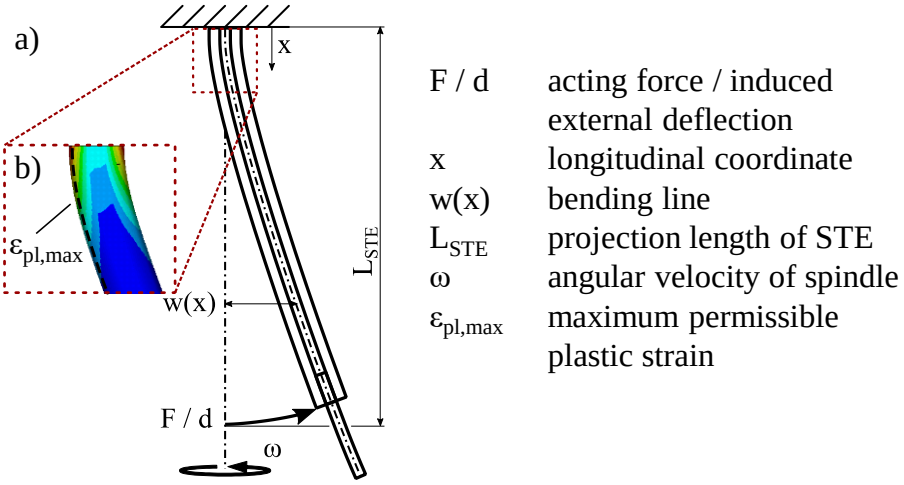

Fig. 10. Schematic representation of the FE-model; a) resulting bending line w(x) due to action of a single force F; b) zone in which the maximum permissible plastic strain $\varepsilon_{pl,max}$ is reached

The model was subsequently used to predict the plastic deformation and bending line $w(x)$ for a maximum permissible plastic strain $\varepsilon_{\mathrm{pl,max}}$ in the cantilever's extreme fibre, at the point where the STE is clamped rigidly into the tool holder. The deformation was applied by a singular force F represented by an external deflection d at the free end of the STE, as depicted in Fig.10.

Based on the calculated bending line $w(x)$ the kinetic energy E_{kin} of the deformed STE was calculated for a critical spindle speed n_{crit} and compared to safety levels of safeguards provided by ISO 14120 [48]. The results in Fig. 11 show the results of the analysis. The results in Fig. 11 clearly show that STE with an outer diameter of $d_{STE} \geq 15$ mm reach critical levels of kinetic energy E_{kin} according to ISO 14120 [48]. Various defined safety levels such as $Y_{pc,4}$ and $Y_{pc,2x6}$ for polycarbonate (PC) vision panels with a thickness of t_{PC} = 4 mm and t_{PC} = 2 x 6 mm, respectively, are exceeded. Thus, the results provide a clear indication of the

inherent hazard potential of STE. Current safeguards do not account for an increased kinetic energy E_{kin} due to an eccentric mass m_{STE} of STE and may not provide sufficient protection to the machine operator in the event of an accident.

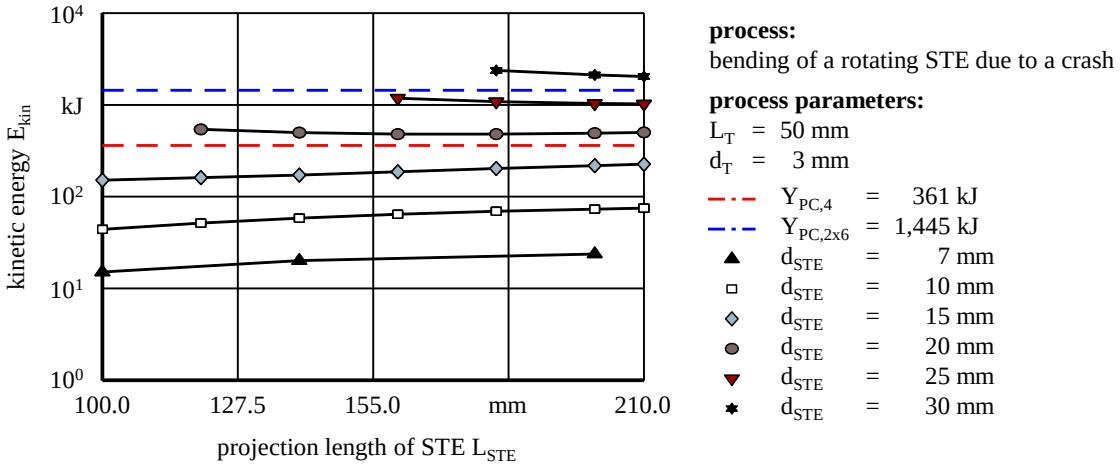

Fig. 11. Representation of the kinetic energy E_{kin} due to plastic deformation at critical spindle speed n_{crit} of STE

Therefore, it is imperative to improve the current safety measures in machine tools in order to keep pace with the continuous increase in productivity.

4.2. NOVEL STATISTICAL APPROACH FOR THE EVALUATION OF IMPACT TESTS

Growing demands for machine safety cannot be met by evaluating potential hazards alone. To cope with the increasing process speeds and higher kinetic energies E_{kin} of moving components in machine tools as productivity increases, it is imperative to also improve protection measures. This includes, in particular, assessing the adequacy of protection provided by safeguards against ejected workpiece r tool fragments. Sufficient protective performance is primarily evaluated by means of impact tests in which a safeguard is subjected to a high-energy impact from a blunt projectile. In accordance with the provisions of international standards such as ISO 14120 [48], the damage pattern of a safeguard is evaluated to assess the impact test result. A test is considered to be passed as long as there are only elastic-plastic deformations with incipient cracks. As soon as the deformation results in a continuous crack that is visible on both sides of the safeguard, the test is considered failed. The highest kinetic energy E_{kin} that a protective device can withstand is referred to as the impact resistance (IR) Y, which serves as a quantitative measure of the protective performance. Traditionally, the IR Y and its associated IR-velocity v_Y are determined using the bisection method. In this method, an interval of projectile velocities v_{pr} is defined, bounded by a lower projectile velocity $v_{pr,low}$ and an upper projectile velocity $v_{pr,up}$, where both quantities satisfy the conditions shown in Eq. (2).

$$v_{pr,low} \leq v_Y \leq v_{pr,up} \tag{2}$$

This initially wide interval allows only an inaccurate determination of the IR-velocity v_Y. For a more precise determination, additional impact tests are carried out with a projectile velocity of $v_{pr,low} < v_{pr} < v_{pr,up}$. If the safeguard passes this test, the projectile velocity v_{pr} of the last test is used as the new lower projectile velocity $v_{pr,low}$ and vice versa. This procedure is repeated until a sufficiently narrow interval is determined. The IR-velocity v_Y is assumed to be found within the identified interval. Since the determination of the IR-velocity v_Y is based on only the last two impact tests, this method is sensitive to variations in the test conditions or the material. Therefore, determining the IR-velocity v_Y is only possible to a limited extent.

In the study of Uhlmann et al. [49] a novel statistical approach was presented that allows to overcome the described limitations of the bisection-method. This approach includes all impact tests of a test series and thus allows a robust and more accurate determination of the IR Y. Although applicable to any type of machine safety device, the statistical approach was originally developed for PC-vision panels. Uhlmann et al. [49] evaluated a total number of n = 105 impact tests conducted at the impact test facility of IWF, see Fig. 12.

A standardized projectile with a mass of m_{pr} = 2.5 kg according to ISO 23125 [50] was used for all impact tests. The velocity of the projectile v_{pr} is controlled by the pressure p_a in the pressure tank and the acceleration length l_a inside the barrel. A light barrier placed behind the muzzle of the barrel is used to measure the projectile velocity v_{pr}. Two high-speed cameras are used to capture the impact process, as illustrated in the snapshots of Fig.12b. Square PC-vision panels with a width of w_{PC} = 300 mm and a thickness of t_{PC} = 12 mm were subjected to a central impact.

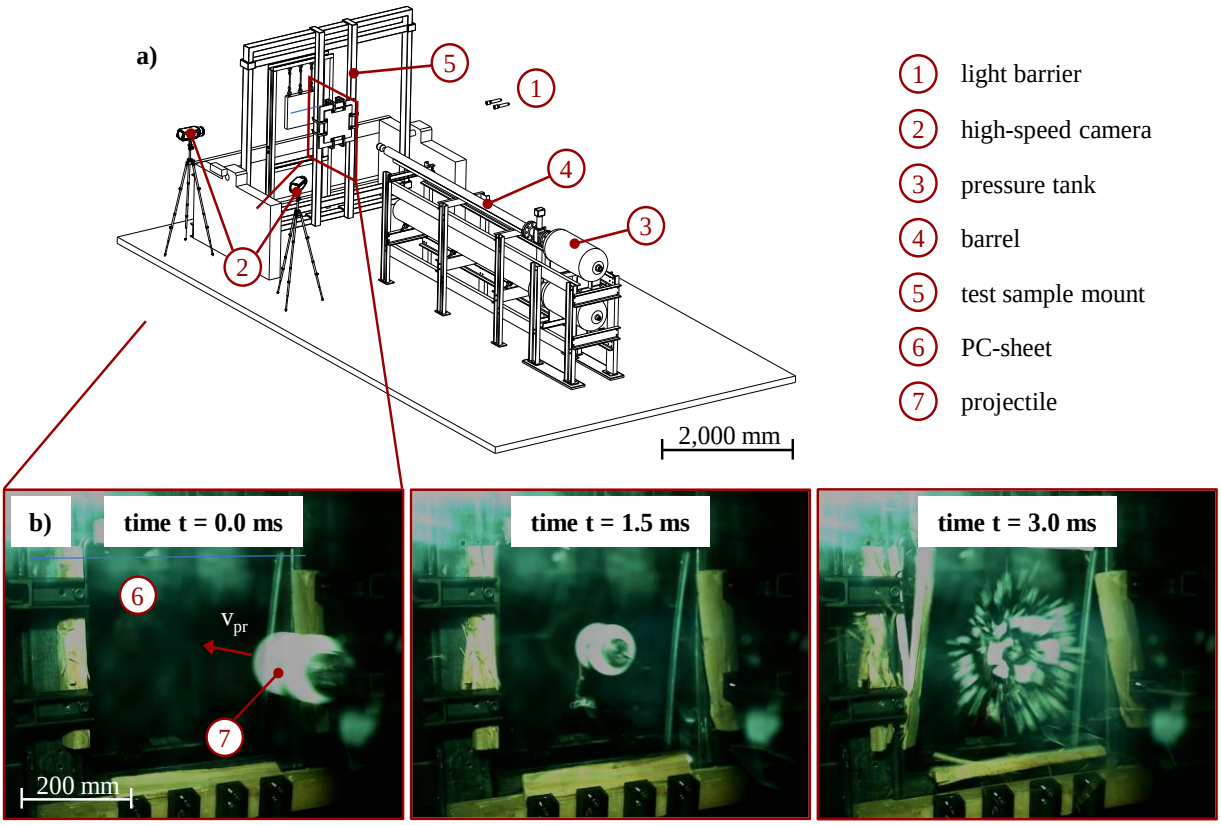

Fig. 12. Impact test facility; a) isometric view of entire test facility; b) snapshots of an impact test

The novel statistical approach is based on the premise that a series of impact tests can be described statistically by a normal distribution [51]. This allows to display the results of the impact tests in the form of a histogram. For this purpose, the kinetic projectile energy E_{pr} of all tests is divided into ranges and the relative frequency h of the event "failed test" is calculated. The relative frequencies h can then be used to obtain a cumulative distribution function (CDF) of a normal distribution. For this purpose, the relative frequencies h are used as grid points to estimate the parameters mean $\overline{x}_y$ and variance s^2 of the CDF by curve fitting algorithms. Figure 13 shows the results of such an analysis.

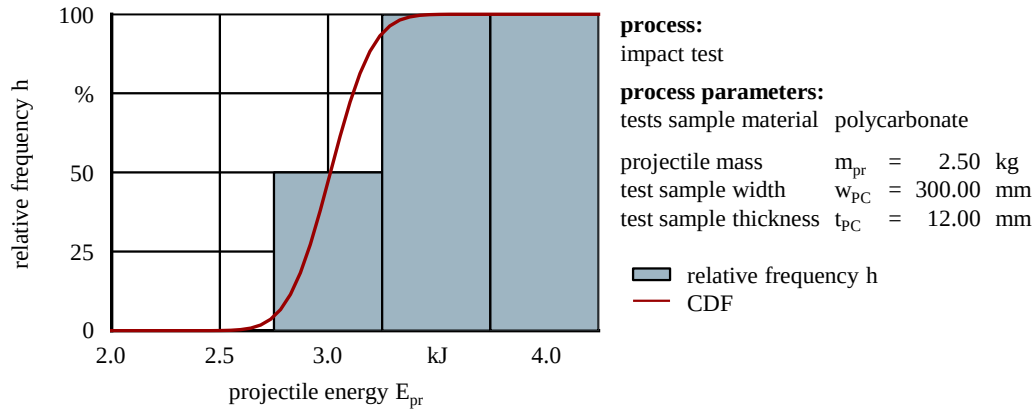

Fig. 13. Relative frequencies h of failed impact tests and the corresponding CDF

It is also possible to derive a probability density function (PDF) from the CDF, which serves as an estimator function for the IR Y in terms of the probability of failed impact tests, as illustrated in Fig. 14.

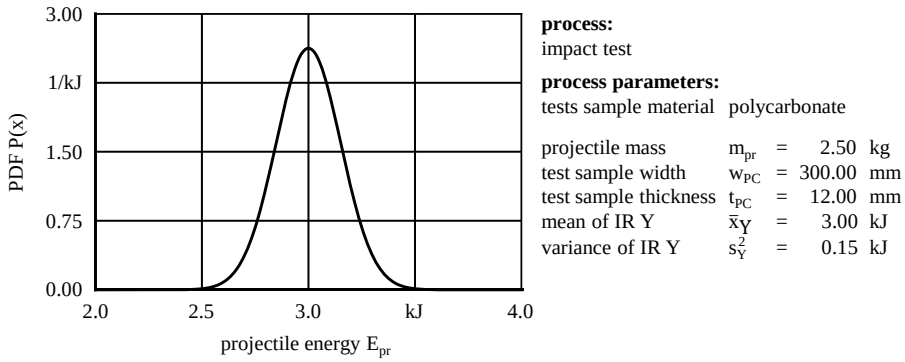

Fig. 14. PDF of failed impact tests

The statistical approach has clear advantages over the common bisection method for determining the IR Y. Unlike the conventional method, all test results are included in the determination of the IR Y, which increases its reliability. Knowledge of the IR Y as a statistically scattering quantity with a mean $\overline{x}_y$ and a variance s_Y^2, allows a more accurate assessment of the protective performance of the safeguards. The novel approach helps to meet the challenges posed by measures taken to improve the productivity of machine tools.

5. SUMMARY AND OUTLOOK

A steadily growing world population and the continuing trend toward urbanization require efficient use of available resources and high levels of productivity. In terms of production factors, productivity can be defined by an output-input ratio. A high level of productivity is accomplished by maximizing the output while minimizing the input. This paper discusses approaches to both challenges. For example, using a thermoelectric temperature control system for motorized milling spindles to precisely control the temperature of machine tools maximizes output. The implemented system allowed a significant reduction of the auxiliary process time due to shorter warm-up times t_W, thus increasing productivity. Another approach focuses on using industrial robots in manufacturing processes that require high accuracy. An AI-based compensation for tool displacement was presented, providing a means to overcome the current precision limitations of industrial robots. In addition to industrial robots, the potential of modularized machine tool frames is presented. Configured on demand, such modularized frames enhance both flexibility and resource efficiency, contributing significantly to an increase in productivity.

However, high productivity in terms of HPC and HSC comes with a substantial increase in energy consumption. In this context, the tempering of machine tools is of particular importance. Means to mitigate the increased energy consumption by tempering with a self-sufficient TEG-based cooling system for LDD are presented. In this case, productivity is improved by minimizing the energy usage.

In addition, the implications in terms of machine safety associated with measures to increase productivity, such as HPC and HSC machining, are highlighted. Elevated hazard potentials due to the application of STE are identified by a model-based analysis. On the protection side a novel statistical model is presented allowing to assess the protective performance of safeguards more accurately. The cutting-edge technologies presented contribute to the future advancement of machine tools.

ACKNOWLEDGEMENTS

The author would like to thank all the researchers who contributed to this paper, in particular Dr.-Ing. Mitchel Polte, Julian Blumberg, Florian Triebel, Nils Bergström, and Jan Streckenbach.Also, the author would like to thank the Deutsche Forschungsgemeinschaft (German Research Foundation) for funding this research within the Sonderforschungsbereich 1026 (Collaborative Research Centre 1026) and UH100/195-2.Furthermore, a large part of the results presented have been achieved in the projects "Roboterbasiertes Kragenziehen" (Ref.-No. AiF 20457BG), "Sicherheit schlanker Werkzeugverlängerungen" (Ref.-No. VDW-FI-Nr. 030), and "KSS-PC" (Ref.-No. VDW-FI-Nr. 028), which were financed and supervised by the European Research Association for Sheet Metal Working (EFB) and the German Machine Tool Builders'Association (VDW), respectively. They were supported by the German Federation of Industrial Research Associations (AiF) in its Industrial Collective Research program funded by the Federal Ministry of Economic Affairs and Climate Action (BMWK). The project „TubuPELT" is supported by the Federal Ministry for Economic Affairs and Climate Action (BMWK) on the basis of a decision by the German Bundestag.

REFERENCES

[1] https://www.statista.com/chart/28744/world-population-growth-timeline-and-forecast/ (Access: 21/03/2023).
[2] https://www.statista.com/topics/9350/urbanization/#topicOverview (Access: 21/03/2023).

[3] https://www.statista.com/statistics/263437/global-smartphone-sales-to-end-users-since-2007/(Access:21/03/2023).
[4] https://de.statista.com/statistik/daten/studie/309656/umfrage/prognose-zur-anzahl-der-smartphone-nutzer-weltweit / (Access: 21/03/2023).
[5] JEDRZEJEWSKI J., KWASNY W., 2011, *Study on Reducing Energy Consumption in Manufacturing Systems*, Journal of Machine Engineering 11/3, 7–20.
[6] MAYR J., JEDRZEJEWSKI J., UHLMANN E., ALKAN DONMEZ M., KNAPP W., HÄRTIG F., WENDT K., MORIWAKI T., SHORE P., SCHMITT R., BRECHER C., WÜRZ T., WEGENER K., 2012, *Thermal Issues in Machine Tools*, CIRP Annals 61/2, 771–791.
[7] UHLMANN E., MULLANY B., BIERMANN D., RAJURKAR K.P., HAUSOTTE T., BRINKSMEIER E., 2016, *Process Chains for High-Precision Components with Micro-Scale Features*, CIRP Annals – Manufacturing Technology 65, 549–572.
[8] BRECHER C., WECK M., 2021, *Machine Tools Production Systems 2: Design, Calculation and Metrological Assessment*, Springer-Verlag GmbH, Berlin.
[9] UHLMANN E., HEITMÜLLER F., MATHEI M., REINKOBER S., 2013, *Applicability of Industrial Robots for Machining and Repair Processes*, Procedia CIRP 11, 234–238.
[10] https://unfccc.int/sites/default/files/english_paris_agreement.pdf (Access: 21/03/2023).
[11] FENG C., HUANG S., 2020, *The Analysis of Key Technologies for Sustainable Machine Tools Design*. Applied Sciences 10, 731.
[12] UHLMANN E., LANG K.-D., PRASOL L., THOM S., PEUKERT B., BENECKE S., WAGNER E., SAMMLER F., RICHARZ S., NISSEN N.F., 2017, *Sustainable Solutions for Machine Tools*, Sustainable Manufac., 2, 47–69.
[13] SHABI L., WEBER J., WEBER J., 2017, *Analysis of the Energy Consumption of Fluidic Systems in Machine Tools*, Procedia CIRP 63, 573–579.
[14] https://sdgs.un.org/goals (Access: 21/03/2023).
[15] DENKENA B., BERGMANN B., KLEMME H., 2020, *Cooling of Motor Spindles–a Review*, The International Journal of Advanced Manufacturing Technology, 110, 3273–3294.
[16] JONATH L., LUDERICH J., BREZINA J., GONZALEZ DEGETAU A.M., KARAOGLU S., 2023, *Improving the Thermal Behavior of High-Speed Spindles Through the Use of an Active Controlled Heat Pipe System*, 3rd International Conference on Thermal Issues in Machine Tools.
[17] UHLMANN E., POLTE J., SALEIN S., IDEN N., TEMME P., HARTUNG D., PERSCHEWSKI S., 2020, *Development of a Thermoelectrically Tempered Motorised Spindle*, wt Werkstattstechnik online 110/5, 299–305.
[18] LAI C.Y., VILLACIS CHAVEZ D.E., DING S., 2008, *Transformable Parallel-Serial Manipulator for Robotic Machining*, The International Journal of Advanced Manufacturing Technology 97/5–8, 2987–2996.
[19] FRAUNHOFER SOCIETY, 2022, *Flexmatik 4.1*, URL: https://www.flexmatik.de/ (Access: 09/01/2023).
[20] KLIMCHIK A., PASHKEVICH A., 2018, *Robotic Manipulators with Double Encoders: Accuracy Improvement Based on Advanced Stiffness Modeling and Intelligent Control*, IFAC PapersOnLine, 51/11, 740–745.
[21] XIAOYING S., XIAOJUN Z., PENGYUAN W., CHEN H., 2018, *A Review of Robot Control with Visual Servoing*, Proceedings of IEEE 8th Annual Conference on Cyber Technology in Automation, Control and Intelligent Systems, 116–121.
[22] GIERLAK P., 2021, *Force Control in Robotics: A Review of Applications*, Journal of Robotics and Mechanical Engineering 1/1.
[23] KAMALI K., BONEV I.A., 2019, *Optimal Experimental Design for Elasto-Geometrical Calibration of Industrial Robots*, IEEE/ASME Transactions on Mechatronics, 24/6, 2733–2744.
[24] JIANG Z., HUANG M., 2021, *Stable Calibrations of Six-DOF Serial Robots by Using Identification Models with Equalized Singular Values*, Robotica, 39/12, 1–22.
[25] UHLMANN E., POLTE M., BLUMBERG J., ZHOULONG L., KRAFT A., 2021, *Hyperparameter Optimization of Artificial Neural Networks to Improve the Positional Accuracy of Industrial Robots*, Journal of Machine Engineering, 21/2, 47–59.
[26] BLUMBERG J., ZHOULONG L., BESONG L.I., POLTE M., BUHL J., UHLMANN E., BAMBACH M., 2021, *Deformation Error Compensation of Industrial Robots in Single Point Incremental Forming by Means of Data-Driven Stiffness Model*, Proceedings of the 26th International Conference on Automation and Computing, 1–6.
[27] CUI Z., GAO L., 2010, *Studies on Hole-Flanging Process Using Multistage Incremental Forming*, Journal of Manufacturing Science and Technology, 2/2, 124–128.
[28] BESONG L.I., BUHL J., ÜNSAL M., BAMBACH M., POLTE M., BLUMBERG, J., UHLMANN E., 2020, *Development of Tool Paths for Multi-Axis Single Stage Incremental Hole-Flanging*, Procedia Manufacturing 47, 1392–1398.
[29] CHEN X., WEN T., QIN J., HU J., ZHANG M., ZHANG Z., 2020, *Deformation Feature of Sheet Metals During Inclined Hole Flanging by Two Point Incremental Forming*, International Journal of Precision Engineering and Manufacturing 21, 169–176.

[30] KOREN Y., 1999, *Reconfigurable Manufacturing Systems*, CIRP Annals-Manufacturing Technology, 48/2, 527–540.
[31] MORI M., FUJISHIMA M., 2009, *Reconfigurable Machine Tools for a Flexible Manufacturing System*, Changeable and Reconfigurable Manufacturing Systems, Springer, 101–109.
[32] BRANKAMP K., HERRMANN J., 1969, *Baukastensystematik – Grundlagen und Anwendung in Technik und Organisation*, Ind.-Anz., 91, 693–697.
[33] ITO Y., 2008, *Modular Design for Machine Tools*, McGraw Hill Professional.
[34] WULFSBERG J.P., VERL A., WURST K.H., GRIMSKE S., BATHKE C., HEINZE T., 2013, *Modularity in Small Machine Tools*, Production Engineering, 7/5, 483–490.
[35] ABELE E., WÖRN A., 2009, *Reconfigurable Machine Tools and Equipment*, Changeable manufacturing systems, Springer, 111–125.
[36] PEUKERT B., SAOJI M., UHLMANN E., 2015, *An Evaluation of Building Sets Designed for Modular Machine Tool Structures to Support Sustainable Manufacturing*, Procedia CIRP, 26, 612–617.
[37] UHLMANN E., SAOJI M., PEUKERT B., 2016, *Principles for Interconnection of Modular Machine Tool Frames*, Procedia CIRP, 40, 413–418.
[38] UHLMANN E., SALEIN S., 2016, *Concepts of Self-Sufficient Cooling Systems for Linear Direct Drives*, Zeitschrift für wirtschaftlichen Fabrikbetrieb, 111/7–8, 411–415.
[39] UHLMANN E., SALEIN S., 2017, *Experimental Investigation of Self-Sufficient Cooling Systems for linear Direct Drives of Machine Tools*, wt Werkstattstechnik online, 107/5, 359–365.
[40] UHLMANN E., PRASOL L., THOM S., SALEIN S., WIESE R., 2018, *Development of a Dynamic Model for Simulation of A Thermoelectric Self-Cooling System for Linear Direct Drives In Machine Tools*, Proceedings of 1th Conference on Thermal Issues in Machine Tools, Wissenschaftliche Scripten, Dresden, 75–91.
[41] UHLMANN E., POLTE M., SALEIN S., TRIEBEL F., IDEN N., 2019, *Adaptive Cooling System with Thermoelectric Generators*, Zeitschrift für wirtschaftlichen Fabrikbetrieb, 114/11, 757–762.
[42] UHLMANN E., SALEIN S., POLTE M., TRIEBEL F., 2020, *Modelling of a Thermoelectric Self-Cooling System Based on Thermal Resistance Networks for Linear Direct Drives In Machine Tools*, Journal of Machine Engineering 20/1, 43–57.
[43] UHLMANN E., SALEIN S., 2022, *Performance Analysis of an Adaptive Cooling System with Primary and Secondary Heat Paths for Linear Direct Drives in Machine Tools*, CIRP Journal of Manufacturing Science and Technology, 39, 91–103.
[44] SCHNEIDER M., MICHELBERGER M., 2017, *Schlanke Spannlösungen Erleichtern die Zugänglichkeit,* VDI-Z Special Werkzeuge + Fertigungstechnik 1, Springer-VDI, Düsseldorf.
[45] HENNING F., MOELLER E., 2011, *Handbuch Leichtbau*, Carl Hanser, München.
[46] DIN 69882-8, 2005, *Werkzeughalter mit kegel-hohlschaft*, Beuth, Berlin.
[47] THOM S., UHLMANN E., 2019, *Safety of Slim Tool Extensions for Milling Operations at the Limit, Wissenschaftliche Gesellschaft für Produktionstechnik*, 9/2, 347–356.
[48] DIN EN ISO 14120, 2015, *Safety of Machinery - Guards - General Requirements for Design and Construction of Fixed and Movable Guards*, ISO copyright office, Vernier.
[49] UHLMANN E., POLTE M., BERGSTRÖM N., MÖDDEN H., 2022, *Analysis of the Effect of Cutting Fluids on the Impact Resistance of Polycarbonate Sheets by Means of a Hypothesis Test*, Proceedings of the 32nd European Safety and Reliability Conference (ESREL 2022), 2358–2365.
[50] ISO 23125, 2015, *Machine Tools – Safety – Turning Machines*, ISO Copyright Office, Vernier.
[51] MÖDDEN H., BERGSTRÖM N., 2022, *Design of Impact Tests for Polycarbonate Sheets and Their Deterioration by Cooling Lubricants – Part 1: Models and Limitations of Measurement*, Proceedings of the 32nd European Safety and Reliability Conference (ESREL 2022), 2350–2357.